UDC 678.746.2:544.77:620.22-022.532

Nafisa Ergasheva [a], Gulnora Ikhtiyarova [b], Gulchexra Ikhtiyarova [a], Dilnoza Isomitdinova [b]

PHYSICOCHEMICAL STUDIES OF THE STRUCTURE OF CHITOSAN AND NANOCHITOSAN FROM *APIS MELLIFERA*

[a] Bukhara State Medical Institute, Bukhara, Uzbekistan
[b] Tashkent State Technical University, Tashkent, Uzbekistan

This study investigates the extraction of chitosan from *Apis mellifera* biomass and the synthesis of nanochitosan by ionic gelation combined with ultrasonication. Chitosan was obtained through microwave-assisted deacetylation of chitin isolated from dried honeybee exoskeletons, yielding a product with a molecular weight of 103 kDa and a degree of deacetylation of approximately 80%. Nanochitosan was prepared by crosslinking chitosan with sodium tripolyphosphate in an acidic medium, followed by ultrasonic treatment. Dynamic light scattering analysis showed a decrease in Z-average particle size from 305.9 nm for chitosan to 170.2 nm for nanochitosan, confirming successful nanoparticle formation. However, the high polydispersity index (1.831) indicated considerable aggregation and the need for further optimization of synthesis conditions. Fourier transform infrared spectroscopy confirmed preservation of the main chitosan structure, while spectral changes in the 1550−1600 cm^{-1} and 1240−1260 cm^{-1} regions verified ionic crosslinking with sodium tripolyphosphate. Scanning electron microscopy revealed a porous hierarchical morphology, and energy-dispersive X-ray spectroscopy confirmed the elemental composition and the presence of phosphorus, supporting successful crosslinking. Overall, *Apis mellifera* is a promising sustainable source of chitosan, and the proposed synthesis approach yields nanochitosan with favorable physicochemical properties for pharmaceutical and biomedical applications.

Keywords: nanochitosan, *Apis mellifera*, microwave-assisted, ionic gelation, sodium tripolyphosphate, ultrasonication, polydispersity, Fourier transform infrared spectroscopy, scanning electron microscopy, dynamic light scattering.

DOI: 10.32434/0321-4095-2026-167-4-166-177

Introduction

Among nanomaterials derived from biopolymers, chitosan has particular scientific and practical significance. Chitosan (CS) is a natural polysaccharide obtained by the alkaline deacetylation of chitin, and it is found in the cellular structure of crustaceans, insects, fungi, and certain microorganisms [1−3].

When the degree of deacetylation of chitin reaches about 50% (depending on the origin of the polymer), it becomes soluble in aqueous acidic media and is called chitosan. Chitosan is the only pseudonatural cationic polymer and thus, it finds many applications that follow from its unique character (flocculants for protein recovery, depollution, etc.) [4].

Chitosan is derived from naturally occurring sources, which is the exoskeleton of insects, crustaceans

and fungi that has been shown to be biocompatible and biodegradable. Chitosan is a linear copolymer of β-(1→4)-linked 2-amino-2-deoxy-D-glucopyranose and 2-amino-2-deoxy-D-glycopyranose. It is obtained by deacetylation of its parent polymer chitin, a polysaccharide widely distributed in nature [1].

Chitosan is an N-deacetylated derivative of chitin obtained by transforming the acetamide groups into primary amino groups. However, deacetylation of chitin is almost never complete and chitosan or deacetylated chitin still contains acetamide groups to some extent. Unlike cellulose, chitin and chitosan contain 5–8% nitrogen, which in chitin is in form of acetylated amine groups and in chitosan in form of primary aliphatic amine groups, which makes chitin and chitosan suitable for typical reactions of amines [2].

Nanotechnology has enabled the design of materials and systems capable of interacting with biological structures at the molecular level, which is especially important in modern biomedical applications [5–7].

From a physicochemical point of view, chitosan has the special quality of gelling upon contact with anions thus allowing the formation of beads under very mild conditions. These CS beads showed a pH-dependent swelling behavior, which makes them appropriate for the delivery of drugs in the gastric cavity. Nevertheless, due to their large size (1–2 mm), these beads are not appropriate for other routes of administration, such as those which require injection or deposition in mucosal surfaces (nasal, mucosal). The reduction of the size of CS particles down to the nanometers range was achieved. However, an important drawback of these nanoparticles is that they were prepared by a crosslinking reaction with the potentially antigenic agent glutaraldehyde [3].

Therefore, in this study, an alternative and safer approach was employed for nanoparticle synthesis, namely the ionic gelation method, in which chitosan was cross-linked with sodium tripolyphosphate (TPP) to obtain nanochitosan. The main advantage of this method is that it does not require the use of toxic and potentially antigenic agents such as glutaraldehyde and can be carried out under mild conditions. In addition, the nanochitosan particles formed using TPP exhibit a high surface-to-volume ratio, which significantly enhances their biological activity, stability, and drug encapsulation capacity. In this context, chitosan-based nanomaterials have attracted considerable attention as promising carriers for drug delivery due to their biocompatibility and functional versatility [8].

Microwave-assisted deacetylation and ultrasonication are considered effective approaches for improving chitosan processing, reducing reaction time, and promoting particle size reduction and system stability [9–11].

A general comparison of methods for obtaining chitosan and nanochitosan is given in Tables 1 and 2, respectively.

Various methods have been employed for the preparation of nanochitosan, including chemical approaches such as emulsification, precipitation, ionic gelation, and covalent or ionic crosslinking, as well as physical methods such as ultrasonication and microwave treatment [12].

Owing to its nanoscale structure, nanochitosan demonstrates significantly improved physicochemical properties compared to bulk chitosan. In particular, the reduction in particle size to the nanometer scale leads to an increased surface-to-volume ratio, which enhances its reactivity, adsorption capacity, and interaction with biological systems [13].

Furthermore, nanochitosan is typically positively charged, enabling effective interaction with negatively charged cell membranes [8]. The transition to the nanoscale also improves its solubility, especially in acidic media, where its dispersion is enhanced [2].

The source of raw materials and the initial processing methods play a crucial role in chitosan production. Traditionally, chitosan is primarily

Table 1

Laboratory methods for the extraction of chitosan from chitin

Method	Brief description	Advantages	Disadvantages
Chemical method	Chitosan is obtained from chitin using alkaline solutions	Fast and simple	Environmental impact, possible chemical residues
Biological method (enzymatic/biological)	Chitosan is produced from chitin using enzymes or bacteria	Eco-friendly, high-quality product	Time-consuming, expensive enzymes
Physical method (microwave-assisted, ultrasonic)	Chitosan deacetylation is accelerated using microwaves or ultrasound	Fast and effective	Equipment is expensive

obtained from marine crustaceans; however, in recent years, there has been an increasing need to explore alternative and locally available sources due to ecological and economic considerations [14].

In this regard, biological waste from *Apis Mellifera* (honeybees) has been identified as a promising source for chitin and chitosan extraction, as insect exoskeletons contain a significant amount of chitin. Chitin and chitosan derived from various biological sources, including fishery waste and insects, have attracted considerable attention due to their biodegradability and versatile applications. In particular, chitin and chitosan obtained from *Apis mellifera* have been reported to exhibit valuable physicochemical properties, making them promising for biomedical and environmental applications [15].

Recent studies have also demonstrated that chitosan-based materials can be applied in textile processing and wastewater treatment, including sorbent systems based on *Apis Mellifera* chitosan combined with bentonite or vermiculite [15].

The aim of this study is to extract chitosan from *Apis Mellifera* sources using various methods, to synthesize nanochitosan via ionic gelation combined with ultrasonic treatment, and to analyze its physicochemical properties (particle size, structure, and stability). The results demonstrate that nanochitosan is an environmentally friendly material with significant potential for applications in various fields.

Materials and methods

Dead *Apis Mellifera* bees collected from local beehives were used as the raw material for this study. Sodium hydroxide (NaOH), hydrochloric acid (HCl), sodium tripolyphosphate (TPP), and acetic acid (CH_3COOH) of analytical grade were used without further purification. All solutions were prepared using distilled water.

All experiments were performed in quadruple, and the average values were reported. The chitosan used for nanochitosan preparation had an average molecular weight of 103 kDa and a degree of deacetylation (DD) of approximately 80%.

The study scheme is shown in Fig. 1. To extract chitin from *Apis Mellifera* samples, the collected bees were first dried and ground into a fine powder. Demineralization was carried out using 5% HCl solution for 1 hour at room temperature. Deproteinization was performed with 7% NaOH solution for 2 hours. The obtained chitin was thoroughly washed with distilled water and dried for further processing.

Table 2

Nanochitosan production methods

Method	Brief description	Advantages	Disadvantages
Ionic gelation	Chitosan reacts with TPP to form nano-sized particles	Simple, clean, effective	Particle size may vary, aggregation possible
Emulsification	Chitosan solution forms an emulsion to produce nanoparticles	Can produce very small particles	Complex process, requires multiple reagents
Spray drying	Chitosan solution is dried to form nanopowder	Suitable for scale-up, widely used	High energy consumption, possible aggregation
Ultrasonic treatment	Ultrasound reduces particle aggregation and size	Reduces aggregation, helps uniform size	Equipment cost, optimization needed
Nanoprecipitation	Chitosan is precipitated in a non-solvent to form nanoparticles	Simple, no surfactant needed	Particle size control can be difficult
Microemulsion	Chitosan is encapsulated in microemulsion droplets to form nanoparticles	Produces uniform particles	Requires surfactants, complex formulation
Self-assembly	Chitosan chains self-assemble into nanoparticles under specific conditions	No harsh chemicals	Process sensitive to pH and ionic strength
Crosslinking	Chemical crosslinkers stabilize chitosan nanoparticles	Stable particles, controlled release possible	Use of chemicals, potential toxicity

The conversion of chitin into chitosan was performed using microwave-assisted treatment. For this purpose, chitin was treated with 50% NaOH solution in a microwave oven for 3 hours. During this process, the deacetylation of chitin was accelerated, resulting in the formation of chitosan. After completion of the reaction, the product was washed several times with distilled water to remove residual alkali and then dried.

The obtained chitosan had a molecular weight of 103 kDa and a degree of deacetylation (DD) of 80%.

Nanochitosan was prepared using the ionic gelation method. Briefly (Fig. 2), chitosan with an average molecular weight of 103 kDa and a degree of deacetylation of 80% was dissolved in 20 mL of 1% acetic acid solution and allowed to stand for 24 hours to ensure complete dissolution. The pH of the solution was adjusted to 5.5 using NaOH solution, while avoiding significant changes in the total volume.

Separately, 0.02 g of sodium tripolyphosphate was dissolved in 10 mL of distilled water (2 mg/mL). The TPP solution was then added dropwise to the chitosan solution under magnetic stirring at 800 rpm for 1 hour. The ionic gelation process was carried out at room temperature (25^{0}C). The mass ratio of chitosan to TPP (XZ:TPP) was maintained at 1:1.

The resulting suspension was subjected to ultrasonic treatment using a GT SONIC Professional Ultrasonic Cleaner at a frequency of 40 kHz for 1.5 hours. During the process, the temperature was maintained below 30^{0}C. To control the temperature, external cooling using ice was applied.

The cavitation effect generated by ultrasonication reduced particle aggregation and promoted the formation of stable nanochitosan particles with a narrower size distribution.

The nanochitosan suspension was centrifuged at 4000 rpm for 15 minutes. The obtained precipitate was filtered through a coarse filter and washed with distilled water. The sample was then dried in an oven at 40^{0}C until a constant weight was achieved.

Various instrumental analysis techniques were employed to determine the structural and physicochemical properties of nanochitosan. The presence of functional groups and the efficiency of the deacetylation process were analyzed using Fourier Transform Infrared Spectroscopy (FTIR). FTIR spectra were recorded within an appropriate range, and the characteristic absorption peaks of chitosan and nanochitosan were analyzed.

The particle size, size distribution, and polydispersity index (PDI) of nanochitosan were determined using Dynamic Light Scattering (DLS). Measurements were carried out at room temperature for samples in colloidal solution, and the average hydrodynamic diameter values were calculated.

Results and discussion

Although chitosan and its nanoscale form are based on the same polysaccharide structure, their physicochemical properties differ significantly. This difference is primarily associated with the reduction in particle size, structural compaction, and the ionic crosslinking process.

The obtained chitosan had an average molecular weight of 103 kDa and a degree of deacetylation of 80%, forming a linear polymer structure in solution. Such a structure tends to aggregate due to intermolecular hydrogen bonding and electrostatic interactions, resulting in a heterogeneous system with a broad size

Fig. 1. Laboratory scheme for the extraction of chitosan from chitin

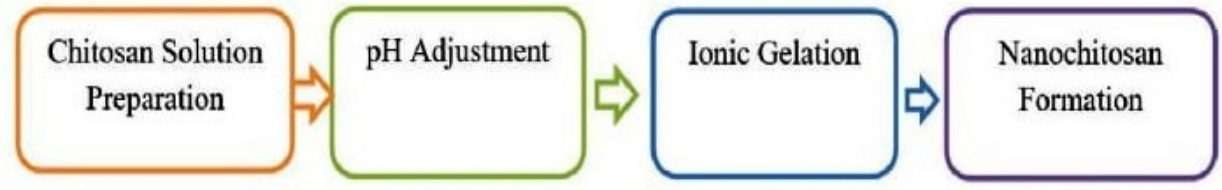

Fig. 2. Laboratory scheme for the preparation of nanochitosan from chitosan

distribution.

In contrast, during the ionic gelation process, negatively charged phosphate groups of sodium tripolyphosphate interact electrostatically with the protonated amino groups of chitosan, forming a three-dimensional crosslinked network structure. Ultrasonic treatment further promotes particle fragmentation and leads to a more compact structure due to cavitation effects.

As a result of particle size reduction (Fig. 3), nanochitosan exhibits a higher surface-to-volume ratio, which enhances its surface reactivity and interaction with biological systems. Therefore, nanochitosan is considered a promising material for pharmaceutical and biomedical applications.

In this study, the particle size distribution and polydispersity index (PDI) of chitosan obtained from Apis mellifera (honeybee) chitin, as well as nanochitosan synthesized from this chitosan, were analyzed using the Dynamic Light Scattering (DLS) technique (Table 3). DLS is an effective method for characterizing particle size in colloidal systems, particularly for evaluating the aggregation behavior of chitosan and nanochitosan.

The Z-average value of the chitosan sample was found to be 305.9 nm. The polydispersity index (PDI) was 0.503, indicating a moderately polydisperse system. The presence of multiple peaks in the DLS spectrum confirms the tendency of chitosan chains to aggregate. The appearance of larger fractions can be explained by intermolecular interactions and chain entanglement within the polymer system.

The obtained DLS results (Fig. 4, Table 4) revealed that the particles were distributed across multiple peaks, indicating the polydisperse nature of the nanochitosan system. According to the number-based distribution, the main fraction was observed at the first peak with an area contribution of 0.731. In this peak, the average hydrodynamic diameter of the particles was approximately 182.2 nm, confirming the formation of nanochitosan. The peak position at around 88.03 nm suggests the presence of relatively small and stable particles within the system.

The second peak, with an area fraction of 0.214, corresponds to larger particles or partially aggregated nanochitosan structures. In this fraction, the average particle size reached 7820 nm, indicating the presence of aggregates formed during the synthesis process. The high standard deviation further confirms that the system is not fully monodisperse.

The third peak, although having a small fraction (0.056), represents the presence of very large clusters. These particles are likely formed due to secondary aggregation during drying, dispersion, or measurement processes.

After ionic gelation and ultrasonic treatment, the Z-average value of nanochitosan was determined to be 170.2 nm. This reduction in particle size reflects the compaction of chitosan chains as a result of crosslinking.

The decrease in particle size from 305.9 nm (chitosan) to 170.2 nm (nanochitosan) confirms the efficiency of the ionic gelation process (Table 5). The electrostatic interactions between TPP and chitosan contribute to the condensation and stabilization of the polymer structure.

The obtained results confirm that nanoscale particles can be successfully produced from chitosan

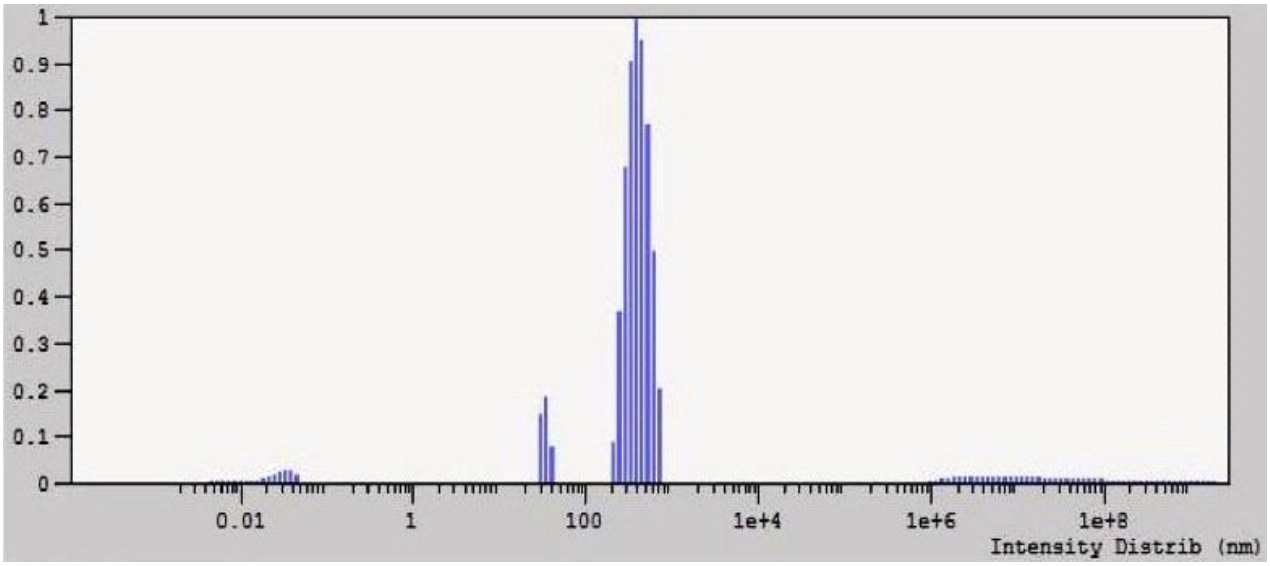

Fig. 3. Particle size distribution of chitosan derived from Apis Mellifera

Table 3

Particle size and distribution parameters of chitosan obtained from DLS analysis

Peak number	Area	Mean	Position	STD
1	0.017	0.032	0.033	0.009
2	0.066	32.55	34.24	6.941
3	0.892	401.0	385.1	138.4
4	0.025	$5.9 \cdot 10^6$	$3.9 \cdot 10^6$	$3.4 \cdot 10^6$

Table 4

Particle size and distribution parameters of nanochitosan obtained from DLS analysis

Peak number	Area	Mean (nm)	Position (nm)	STD (nm)
1	0.731	182.2	88.03	150.3
2	0.214	7820	7074	3404
3	0.056	$2.4 \cdot 10^6$	$1.2 \cdot 10^6$	$2.1 \cdot 10^6$

using a combination of ionic gelation and ultrasonic treatment. However, the high polydispersity index indicates the need for further optimization of the synthesis conditions. In future studies, a more uniform and stable nanochitosan system with a narrower size distribution can be achieved by optimizing parameters such as TPP concentration, ultrasonic power, and processing time.

FTIR spectroscopic analysis of chitosan and nanochitosan

Fourier Transform Infrared (FTIR) spectroscopy was employed to identify the functional groups of chitosan and nanochitosan and to confirm structural changes during the ionic gelation process (Fig. 5). The chemical structures of chitosan (XZ) and nanochitosan (NX) samples were analyzed using FTIR spectroscopy. The spectra were recorded in the range of 4000–400 cm^{-1} (Table 6).

Analysis of chitosan (XZ) spectrum

The FTIR spectrum of chitosan exhibited several characteristic absorption peaks: a broad band at 3400–3500 cm^{-1} corresponding to overlapping –OH and –NH stretching vibrations, indicating the presence of hydrogen bonding; peaks at 2920–2850 cm^{-1} assigned to the C–H stretching vibrations; a peak at 1650 cm^{-1} corresponding to the Amide I (C=O) group; and bands in the range of 1590–1560 cm^{-1} attributed to the $-NH_2$ bending vibrations, confirming the deacetylation process. Additionally, peaks in the region of 1150–1020 cm^{-1} were associated with C–O–C stretching and vibrations of the polysaccharide backbone. The presence of characteristic peaks around 1650 and 1590 cm^{-1} is consistent with the reported degree of deacetylation (~80%) of chitosan. The clear presence of amino group-related bands indicates the successful extraction and formation of chitosan.

Analysis of nanochitosan (NX) spectrum

The FTIR spectrum of nanochitosan retained the main characteristic peaks of chitosan, indicating that the primary chemical structure remained unchanged. However, several differences were observed. A broadening of the band in the region around 3400 cm^{-1} was detected, corresponding to the –OH and –NH stretching vibrations, which suggests enhanced hydrogen bonding due to crosslinking. In both samples, peaks around 2920 cm^{-1} were assigned to the C–H stretching vibrations, confirming that the

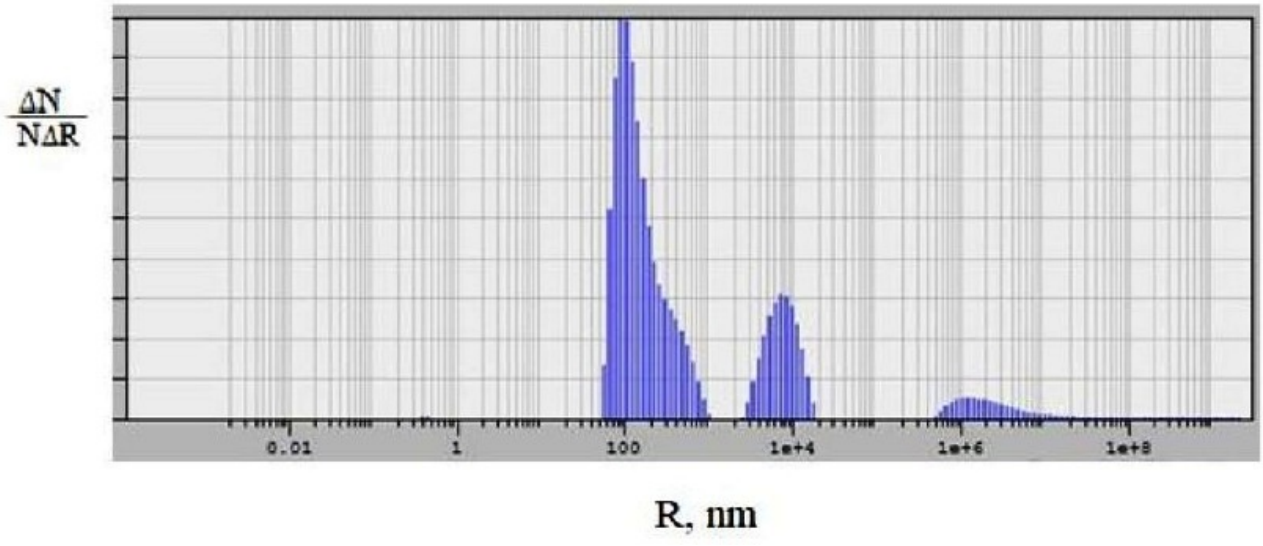

Fig. 4. Particle size distribution of nanochitosan derived from Apis Mellifera

polysaccharide backbone was preserved. The peak at 1650 cm^{-1} (Amide I, C=O) and the band at 1590 cm^{-1} corresponding to the $-NH_2$ bending vibrations were also observed. A noticeable shift in the region of 1550–1600 cm^{-1} indicates electrostatic interactions between chitosan and TPP during ionic gelation. New or intensified peaks observed around 1240–1260 cm^{-1} and 890–900 cm^{-1} correspond to the P=O and P–O bonds, respectively, confirming the interaction between phosphate groups of TPP and the protonated amino groups of chitosan. The bands in the region of 1150–1020 cm^{-1}, associated with the C–O–C and C–O stretching vibrations, indicate the preservation of the polysaccharide structure and the glucosamine ring. Slight changes in peak intensity in nanochitosan are attributed to particle size reduction and structural reorganization.

The FTIR spectra confirm that the main functional groups of chitosan were preserved after nanochitosan formation. The broad band at 3400–3200 cm^{-1} corresponds to the –OH and –NH stretching vibrations. The peaks around 1650 cm^{-1} (Amide I) and 1590 cm^{-1} ($-NH_2$ bending) indicate the partially deacetylated structure of chitosan. Slight shifts and intensity changes observed in the nanochitosan spectrum suggest electrostatic interactions between protonated amino groups of chitosan and TPP during ionic gelation. The retention of bands in the 1150–1020 cm^{-1} region confirms that the polysaccharide backbone remained intact. Overall, the FTIR results verify the successful synthesis of nanochitosan without significant chemical alteration.

These spectral changes provide clear evidence of successful ionic crosslinking and confirm the formation of nanochitosan without significant alteration of the primary polymer structure.

Morphological characteristics of nanochitosan (SEM)

Scanning electron microscopy was employed to evaluate the surface morphology of the synthesized nanochitosan at different magnifications (×500...5000). The obtained micrographs (Fig. 6) clearly demonstrate that the material possesses a non-uniform, irregular morphology with pronounced agglomeration.

Table 5

Comparative analysis of chitosan and nanochitosan

Parameter	Chitosan	Nanochitosan
Z-average* (nm)	305.9	170.2
PDI**	0.503	1.831
Structure	Linear polymer	Cross-linked nanoparticle network
Aggregation	Moderate	High
Surface-to-volume ratio	Lower	Higher

Notes: * – Z-average represents the hydrodynamic diameter of the particles; ** – PDI (polydispersity index) indicates the width of particle size distribution; values close to 0 correspond to monodisperse systems, while values above 0.5 indicate a heterogeneous system.

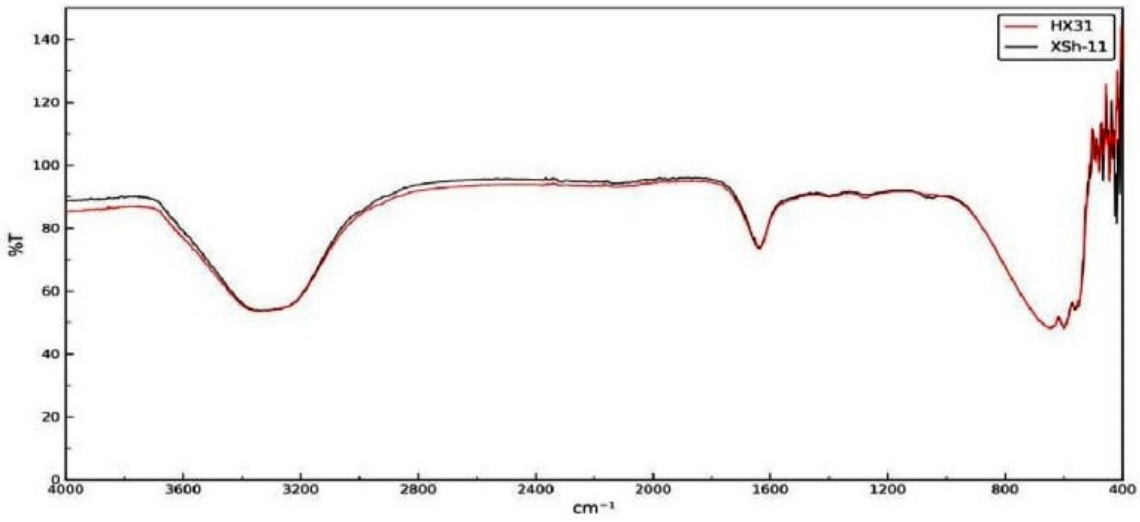

Fig. 5. FTIR spectroscopic analysis of chitosan and nanochitosan

Table 6

Comparative FTIR spectral analysis of chitosan and nanochitosan

Wavenumber (cm^{-1})	XZ (chitosan) characteristics	NX (nanochitosan) characteristics	Functional group/interpretation
3400–3200	Broad and intense peak	Slightly broadened with altered intensity	–OH and –NH stretching vibrations; hydrogen bonding presence
2920–2870	Distinct peak observed	Preserved	C–H stretching vibrations of polysaccharide backbone
1650	Amide I (C=O) band	Reduced intensity or slight shift	Partially deacetylated structure
1590	$–NH_2$ bending vibration	Peak shift or change in shape	Electrostatic interaction with TPP during ionic gelation
1420–1380	CH_2/CH_3 bending vibrations	Preserved	Structural stability of polymer backbone
1150–1020	C–O–C and C–O stretching vibrations	Slight intensity variation	Glycosidic bond structure retained
900–890	β-glycosidic linkage	Preserved	Confirmation of polysaccharide structure

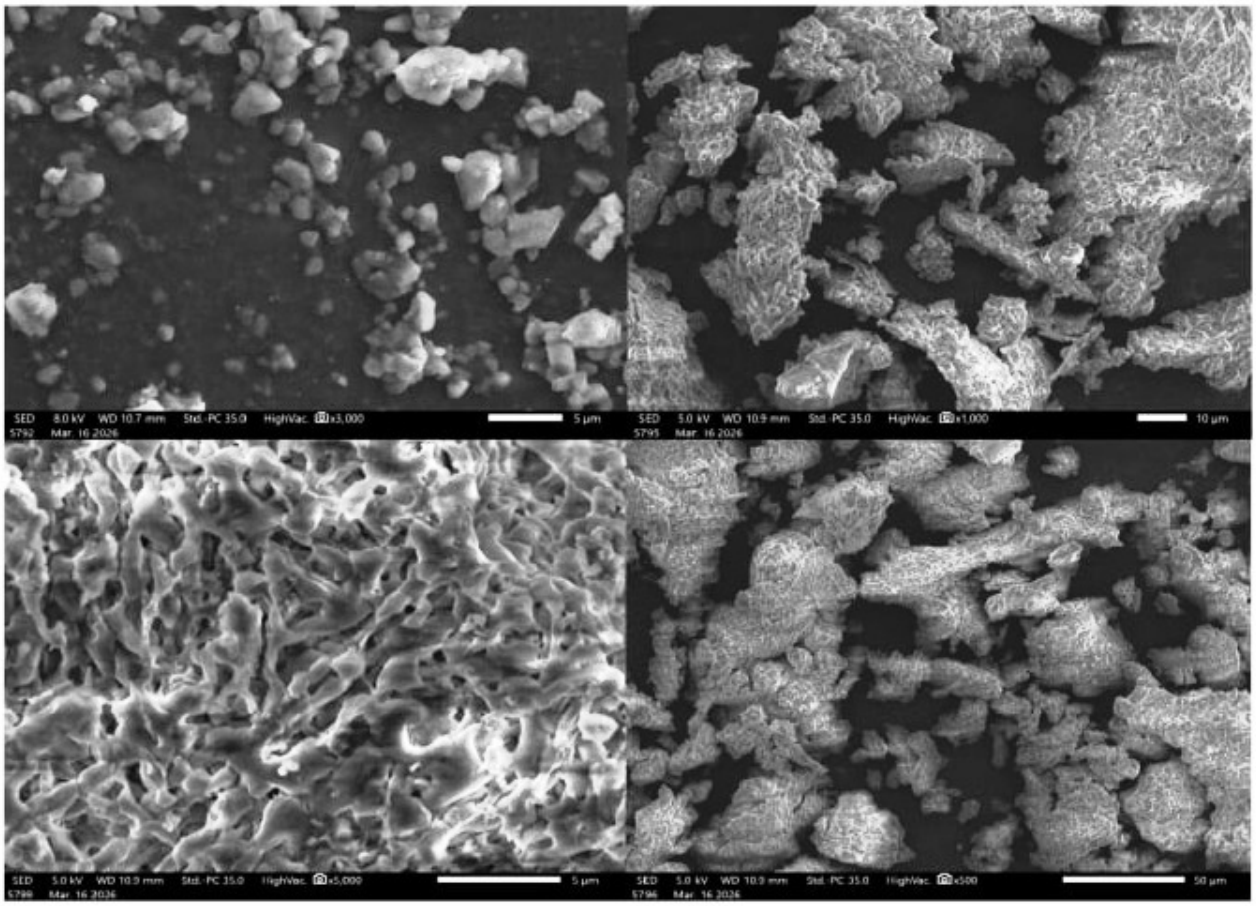

Fig. 6. SEM micrographs of nanochitosan at different magnifications: (a) ×3000; (b) ×1000; (c) ×5000; and (d) ×500, showing agglomerated particles, hierarchical organization, and porous sponge-like morphology

At low magnification (×500), the sample appears as large flake-like aggregates with dimensions reaching up to approximately 50 μm. These structures exhibit rough and folded surfaces, indicating that smaller structural units have coalesced into larger clusters during the drying stage. The absence of discrete particles at this scale suggests the formation of secondary agglomerates rather than isolated entities.

At moderate magnification (×1000...×2000), the morphology becomes more distinguishable, revealing that the large aggregates are composed of smaller substructures with heterogeneous size distribution. The particles are tightly packed, forming compact clusters, which can be attributed to intermolecular hydrogen bonding and electrostatic interactions between chitosan chains after ionic gelation.

At higher magnification (×3000), fine granular domains are observed on the surface of larger aggregates. These domains indicate the presence of primary nano-scale units embedded within micro-scale structures, suggesting the formation of a hierarchical organization. This type of structure is characteristic of nanochitosan synthesized via ionic crosslinking methods.

At the highest magnification (×5000), the material exhibits a highly porous, sponge-like architecture with numerous cavities and interconnected channels. The pore size ranges from submicron to several micrometers. This morphology is indicative of a three-dimensional crosslinked polymer network, which enhances surface area and functional accessibility.

The observed porous structure is strongly influenced by the applied ultrasonic treatment, where cavitation effects generate localized high-energy conditions, leading to:

– disruption of dense polymer regions;
– formation of microvoids and channels;
– increase in surface roughness.

As a result, the synthesized nanochitosan demonstrates a complex hierarchical structure consisting of nano-scale domains aggregated into micro-scale porous clusters.

Elemental composition analysis (EDS)

Energy-dispersive X-ray spectroscopy was performed to determine the elemental composition of the synthesized material (Fig. 7). The quantitative analysis shows that the sample is primarily composed of carbon (≈29%), oxygen (≈41%), and nitrogen (≈27%).

These elements correspond to the fundamental structure of chitosan, which consists of glucosamine units containing hydroxyl and amino functional groups. The relatively high nitrogen content confirms the presence of deacetylated amino groups, characteristic of chitosan. In addition to the main elements, trace amounts of phosphorus, sodium and chlorine were also detected.

The presence of phosphorus is particularly significant, as it confirms the incorporation of tripolyphosphate into the structure. This provides direct evidence of successful ionic crosslinking between protonated amino groups of chitosan and phosphate ions, which is the key mechanism in nanochitosan

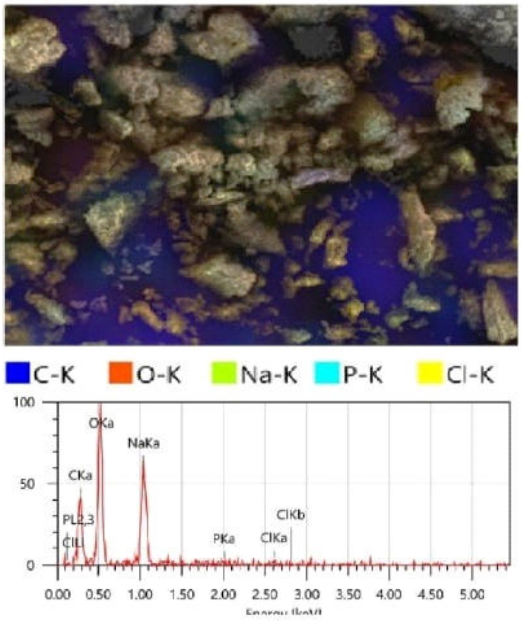

Signal SED
Landing Voltage 10.0 kV
WD 10.8 mm
Magnification x700
Vacuum Mode HighVacuum

Items	Value
measurement conditions	
Acceleration voltage	10.00 kV
Probe current	-
Magnification	x 700
Process time	T3
Measurement detector	First
Live time	30.00 seconds
Real time	30.09 seconds
Dead time	0.00 %
Count rate	75.00 CPS

Display name	Standard data	Quantification method	Result Type
Spc_004	Standardless	ZAF	Metal

Element	Line	Mass%	Atom%
C	K	29.21±1.00	38.75±1.44
O	K	41.57±1.94	41.40±1.93
Na	K	27.56±1.78	19.10±1.23
P	K	0.16±0.37	0.09±0.19
Cl	K	1.47±0.62	0.66±0.28
Total		100.00	100.00
Spc_004			Fitting ratio 0.2212

Fig. 7. EDS mapping, spectrum, and elemental composition of nanochitosan showing C, O, Na, P, and Cl distribution; phosphorus confirms TPP crosslinking

formation. Sodium and chlorine are attributed to residual reagents (NaOH and HCl), indicating minor remnants from the synthesis process.

Elemental mapping analysis

Elemental mapping further supports the EDS findings by illustrating the spatial distribution of elements within the sample. Carbon and oxygen are uniformly distributed across the surface, confirming the homogeneous polysaccharide matrix. Nitrogen is also consistently present, corresponding to the amino functionalities of chitosan.

Phosphorus is detected in localized regions, indicating specific crosslinking sites formed by TPP interaction. This non-uniform distribution is typical for ionically cross-linked systems, where binding occurs at discrete sites along the polymer chains. Sodium and chlorine appear in minimal and scattered regions, confirming that their presence is limited and does not significantly affect the overall structure.

The combined SEM and EDS analyses confirm that the synthesized material exhibits:

– a hierarchical morphology (nano→micro aggregation)

– a highly porous and interconnected structure

– successful ionic crosslinking with TPP.

The agglomerated morphology observed in SEM is consistent with the strong intermolecular interactions inherent to chitosan systems, as well as the effects of solvent removal during drying. Meanwhile, the porous architecture and surface roughness are enhanced by ultrasonic treatment, which plays a crucial role in modifying the structural properties.

Conclusions

In this study, chitosan was successfully extracted from *Apis Mellifera* using microwave-assisted deacetylation, resulting in a product with a molecular weight of 103 kDa and a degree of deacetylation of approximately 80%.

Nanochitosan was effectively synthesized via ionic gelation combined with ultrasonic treatment, leading to a significant reduction in particle size from 305.9 nm to 170.2 nm, confirming the efficiency of the applied method. DLS analysis demonstrated that the obtained nanochitosan system is polydisperse, with a dominant nanoscale fraction (~182 nm), while the presence of larger particles indicates partial aggregation within the system.

FTIR results showed that no new chemical bonds were formed in nanochitosan, and the main functional groups of chitosan were preserved. The observed peak shifts and intensity changes indicate structural modifications caused by ionic gelation and ultrasonic treatment, confirming successful nanochitosan formation. Overall, nanochitosan derived from *Apis Mellifera* can be considered an environmentally friendly and promising material for pharmaceutical and biomedical applications. Further optimization of synthesis conditions is required to achieve a more uniform and stable nanosystem.

The synthesized nanochitosan exhibits a highly porous, irregular, and hierarchical morphology, as confirmed by SEM analysis. The structure consists of nano-scale domains aggregated into micro-scale clusters with interconnected pores and channels. EDS results confirm the presence of characteristic elements (C, O, and N) and verify successful ionic crosslinking through the detection of phosphorus originating from TPP. The combined effects of ionic gelation and ultrasonic treatment contribute to the formation of a structurally complex material with enhanced surface properties.

Conflicts of interest

The authors declare no conflicts of interest.

REFERENCES

1. *Chitosan* – a versatile semi-synthetic polymer in biomedical applications / Dash M., Chiellini F., Ottenbrite R.M., Chiellini E. // Prog. Polym. Sci. – 2011. – Vol.36. – No. 8. – P.981-1014.

2. *Islam S., Bhuiyan M.A.R., Islam M.N.* Chitin and chitosan: structure, properties and applications in biomedical engineering // J. Polym. Environ. – 2017. – Vol.25. – P.854-866.

3. *Novel* hydrophilic chitosan-polyethylene oxide nanoparticles as protein carriers / Calvo P., Remunan-Lopez C., Vila-Jato J.L., Alonso M.J. // J. Appl. Polym. Sci. – 1998. – Vol.63. – No. 1. – P.125-132.

4. *Rinaudo M.* Chitin and chitosan: properties and applications // Prog. Polym. Sci. – 2006. – Vol.31. – No. 7. – P.603-632.

5. *Roco M.C.* Nanotechnology: convergence with modern biology and medicine // Curr. Opin. Biotechnol. – 2003. – Vol.14. – No. 3. – P.337-346.

6. *Bhushan B.* Springer handbook of nanotechnology (3rd edition). – Berlin: Springer, 2010. – 1964 p.

7. *Sahoo S.K., Parveen S., Panda J.J.* The present and future of nanotechnology in human health care // Nanomed. Nanotechnol. Biol. Med. – 2007. – Vol.3. – No. 1. – P.20-31.

8. *Chitosan-based* nanomaterials for drug delivery / Li J., Cai C., Li J., Li J., Li J., Sun T., et al. // Molecules. – 2018. – Vol.23. – Art. No. 2661.

9. *Microwave* technique for efficient deacetylation of chitin nanowhiskers to a chitosan nanoscaffold / Lertwattanaseri T., Ichikawa N., Mizoguchi T., Tanaka Y., Chirachanchai S. // Carbohydr. Res. – 2009. – Vol.344. – No. 3. – P.331-335.

10. *Chitosan* nanoparticles: preparation, size evolution and stability / Rampino A., Borgogna M., Blasi P., Bellich B., Cesaro A. // Int. J. Pharm. – 2013. – Vol.455. – No. 1-2. – P.219-228.

11. *Microwave-assisted* deep eutectic solvent extraction of chitin from crayfish shell wastes for 3D printable inks / Li Z., Li M.C., Liu C., Liu X., Lu Y., Zhou G., et al. // Ind. Crops Prod. – 2023. – Vol.194. – Art. No. 116325.

12. *Kaur S., Dhillon G.S.* Recent trends in biological extraction of chitin from marine shell wastes: a review // Crit. Rev. Biotechnol. – 2015. – Vol.35. – No. 1. – P.44-61.

13. *Kumar M.N.V.R.* A review of chitin and chitosan applications // React. Funct. Polym. – 2000. – Vol.46. – No. 1. – P.1-27.

14. *Muzzarelli R.A.A.* Nanochitins and nanochitosans, paving the way to eco-friendly and energy-saving exploitation of marine resources // Polymer science: a comprehensive reference. – 2012. – P.153-164.

15. *Study* of the antibacterial properties of a composition based on chitosan obtained from dead bees Apis Mellifera / Khaydarova K.A., Nurutdinova F.M., Ikhtiyarova G.A., Khaydarov A.A. // Int. J. Chem. Mater. Sci. – 2022. – Vol.5. – No. 1. – P.1-4.

Received 16.04.2026
Revised 25.05.2026
Accepted 14.07.2026
Published 10.08.2026

ФІЗИКО-ХІМІЧНІ ДОСЛІДЖЕННЯ СТРУКТУРИ ХІТОЗАНУ ТА НАНОХІТОЗАНУ З *APIS MELLIFERA*

Нафіса Ергашева, Гульнора Іхтіярова, Гульчехра Іхтіярова, Ділноза Ісомітдінова

У роботі досліджено одержання хітозану з біомаси *Apis mellifera* та синтез нанохітозану методом іонного гелеутворення у поєднанні з ультразвуковим обробленням. Хітозан одержували шляхом мікрохвильового деацетилювання хітину, виділеного із висушених екзоскелетів медоносної бджоли, що забезпечило отримання продукту з молекулярною масою 103 кДа та ступенем деацетилювання близько 80%. Нанохітозан одержували шляхом зшивання хітозану триполіфосфатом натрію в кислому середовищі з подальшою ультразвуковою обробкою. Аналіз методом динамічного розсіювання світла показав зменшення Z-середнього розміру частинок із 305,9 нм для хітозану до 170,2 нм для нанохітозану, що підтверджує успішне формування наночастинок. Водночас високе значення індексу полідисперсності (1,831) свідчить про значну агрегацію та необхідність подальшої оптимізації умов синтезу. Інфрачервона спектроскопія з перетворенням Фур'є підтвердила збереження основної структури хітозану, тоді як зміни спектрів у діапазонах 1550–1600 $см^{-1}$ та 1240–1260 $см^{-1}$ підтвердили іонне зшивання триполіфосфатом натрію. Сканувальна електронна мікроскопія виявила пористу ієрархічну морфологію, а енергодисперсійна рентгенівська спектроскопія підтвердила елементний склад і наявність фосфору, що свідчить про успішне зшивання. Загалом *Apis mellifera* є перспективним відновлюваним джерелом хітозану, а запропонований підхід до синтезу забезпечує одержання нанохітозану зі сприятливими фізико-хімічними властивостями для фармацевтичних та біомедичних застосувань.

Ключові слова: нанохітозан; *Apis mellifera*; мікрохвильове оброблення; іонне гелеутворення; триполіфосфат натрію; ультразвукове оброблення; полідисперсність; інфрачервона спектроскопія з перетворенням Фур'є; сканувальна електронна мікроскопія; динамічне розсіювання світла.

PHYSICOCHEMICAL STUDIES OF THE STRUCTURE OF CHITOSAN AND NANOCHITOSAN FROM APIS MELLIFERA

*Nafisa Ergasheva [a], Gulnora Ikhtiyarova [b], Gulchexra Ikhtiyarova [a], Dilnoza Isomitdinova [b, *]*

[a] **Bukhara State Medical Institute, Bukhara, Uzbekistan**

[b] **Tashkent State Technical University, Tashkent, Uzbekistan**

[*] **e-mail: isomitdinovadilnoza231@gmail.com**

This study investigates the extraction of chitosan from *Apis mellifera* biomass and the synthesis of nanochitosan by ionic gelation combined with ultrasonication. Chitosan was obtained through microwave-assisted deacetylation of chitin isolated from dried honeybee exoskeletons, yielding a product with a molecular weight of 103 kDa and a degree of deacetylation of approximately 80%. Nanochitosan was prepared by crosslinking chitosan with sodium tripolyphosphate in an acidic medium, followed by ultrasonic treatment. Dynamic light scattering analysis showed a decrease in Z-average particle size from 305.9 nm for chitosan to 170.2 nm for nanochitosan, confirming successful nanoparticle formation. However, the high polydispersity index (1.831) indicated considerable aggregation and the need for further optimization of synthesis conditions. Fourier transform infrared spectroscopy confirmed preservation of the main chitosan structure, while spectral changes in the 1550−1600 cm^{-1} and 1240−1260 cm^{-1} regions verified ionic crosslinking with sodium tripolyphosphate. Scanning electron microscopy revealed a porous hierarchical morphology, and energy-dispersive X-ray spectroscopy confirmed the elemental composition and the presence of phosphorus, supporting successful crosslinking. Overall, *Apis mellifera* is a promising sustainable source of chitosan, and the proposed synthesis approach yields nanochitosan with favorable physicochemical properties for pharmaceutical and biomedical applications.

Keywords: nanochitosan; *Apis mellifera*; microwave-assisted; ionic gelation; sodium tripolyphosphate; ultrasonication; polydispersity; Fourier transform infrared spectroscopy; scanning electron microscopy; dynamic light scattering.

REFERENCES

1. Dash M, Chiellini F, Ottenbrite RM, Chiellini E. Chitosan — a versatile semi-synthetic polymer in biomedical applications. *Prog Polym Sci*. 2011; 36(8): 981-1014. doi: 10.1016/j.progpolymsci.2011.02.001.

2. Islam S, Bhuiyan MAR, Islam MN. Chitin and chitosan: structure, properties and applications in biomedical engineering. *J Polym Environ*. 2017; 25: 854-866. doi: 10.1007/s10924-016-0865-5.

3. Calvo P, Remunan-Lopez C, Vila-Jato JL, Alonso MJ. Novel hydrophilic chitosan-polyethylene oxide nanoparticles as protein carriers. *J Appl Polym Sci*. 1998; 63(1): 125-132. doi:10.1002/(SICI)1097-4628(19970103)63:1<125::AID-APP13>3.0.CO;2-4.

4. Rinaudo M. Chitin and chitosan: properties and applications. *Prog Polym Sci*. 2006; 31(7): 603-632. doi: 10.1016/j.progpolymsci.2006.06.001.

5. Roco MC. Nanotechnology: convergence with modern biology and medicine. *Curr Opin Biotechnol*. 2003; 14(3): 337-346. doi: 10.1016/S0958-1669(03)00068-5.

6. Bhushan B. *Springer handbook of nanotechnology* (3rd edition). Berlin: Springer; 2010. 1964 p. doi: 10.1007/978-3-642-02525-9.

7. Sahoo SK, Parveen S, Panda JJ. The present and future of nanotechnology in human health care. *Nanomed Nanotechnol Biol Med*. 2007; 3(1): 20-31. doi: 10.1016/j.nano.2006.11.008.

8. Li J, Cai C, Li J, Li J, Li J, Sun T, et al. Chitosan-based nanomaterials for drug delivery. *Molecules*. 2018; 23: 2661. doi: 10.3390/molecules23102661.

9. Lertwattanaseri T, Ichikawa N, Mizoguchi T, Tanaka Y, Chirachanchai S. Microwave technique for efficient deacetylation of chitin nanowhiskers to a chitosan nanoscaffold. *Carbohydr Res*. 2009; 344(3): 331-335. doi: 10.1016/j.carres.2008.10.018.

10. Rampino A, Borgogna M, Blasi P, Bellich B, Cesaro A. Chitosan nanoparticles: preparation, size evolution and stability. *Int J Pharm*. 2013; 455(1-2): 219-228. doi: 10.1016/j.ijpharm.2013.07.034.

11. Li Z, Li MC, Liu C, Liu X, Lu Y, Zhou G, et al. Microwave-assisted deep eutectic solvent extraction of chitin from crayfish shell wastes for 3D printable inks. *Ind Crops Prod*. 2023; 194: 116325. doi: 10.1016/j.indcrop.2023.116325.

12. Kaur S, Dhillon GS. Recent trends in biological extraction of chitin from marine shell wastes: a review. *Crit Rev Biotechnol*. 2015; 35(1): 44-61. doi: 10.3109/07388551.2013.798256.

13. Kumar MNVR. A review of chitin and chitosan applications. *React Funct Polym*. 2000; 46(1): 1-27. doi: 10.1016/S1381-5148(00)00038-9.

14. Muzzarelli RAA. Nanochitins and nanochitosans, paving the way to eco-friendly and energy-saving exploitation of marine resources. In: Matyjaszewski K, Moller M, editors. *Polymer science: a comprehensive reference*. Elsevier; 2012. p. 153-164. doi: 10.1016/B978-0-444-53349-4.00257-0.

15. Khaydarova KA, Nurutdinova FM, Ikhtiyarova GA, Khaydarov AA. Study of the antibacterial properties of a composition based on chitosan obtained from dead bees Apis Mellifera. *Int J Chem Mater Sci*. 2022; 5(1): 1-4. doi: 10.21744/ijcms.v5n1.1809.